



ACADÉMIE
DES SCIENCES
INSTITUT DE FRANCE

Comptes Rendus

Chimie


Charly Mve Mfoumou, Pradel Tonda-Mikiéla, Francis Ngoye, Spenseur Bouassa Mouguala, Berthy Lionel Mbouti and Guy Raymond Feuya Tchouya

Removal and adsorption kinetics of copper(II) ions from aqueous media on activated carbon in dynamic adsorption on a fixed-bed column

Volume 27 (2024), p. 141-151

Online since: 19 June 2024

<https://doi.org/10.5802/crchim.285>

 This article is licensed under the
CREATIVE COMMONS ATTRIBUTION 4.0 INTERNATIONAL LICENSE.
<http://creativecommons.org/licenses/by/4.0/>



*The Comptes Rendus. Chimie are a member of the
Mersenne Center for open scientific publishing*
www.centre-mersenne.org — e-ISSN : 1878-1543



Research article

Removal and adsorption kinetics of copper(II) ions from aqueous media on activated carbon in dynamic adsorption on a fixed-bed column

Charly Mve Mfoumou^{Ⓢ,**a,b*}, Pradel Tonda-Mikiéla^{Ⓢ,*a,b*}, Francis Ngoye^{*a*}, Spenseur Bouassa Mouguala^{Ⓢ,*a,b*}, Berthy Lionel Mbouiti^{Ⓢ,*a,b*} and Guy Raymond Feuya Tchouya^{Ⓢ,*a,b*}

^{*a*} Laboratoire de Chimie des Milieux et des Matériaux Inorganiques (LC2MI), URCHI/Université des Sciences et Techniques de Masuku (USTM), BP : 943 Franceville, Gabon

^{*b*} Département de Chimie, Faculté des Sciences/Université des Sciences et Techniques de Masuku (USTM), BP : 943 Franceville, Gabon

E-mail: charly.mvemfoumou@univ-masuku.org (C. Mve Mfoumou)

Abstract. Dynamic adsorption experiments on fixed-bed columns and adsorption kinetics studies of Cu²⁺ in aqueous media, under various experimental conditions, were carried out on activated carbon (AC) prepared using coconut shells from Franceville (Gabon). Results of dynamic adsorption experiments showed that particle size (x) of the column bed, flow rate (D) and bed height (h) influence adsorption capacities at saturation (Q_{sat}) and removal percentages (E) of Cu²⁺ on the prepared AC. The best Q_{sat} and E (52.52 mg/g and 55.02%, respectively) were obtained with $0.01 < x < 0.04$ mm, $D = 2$ mL/min, and $h = 3$ cm, with Cu²⁺ concentration and pH constant at 250 mg/L and 6.5, respectively. The adsorption kinetic studies indicated that the Thomas model and pseudo-first-order kinetic model best describe the adsorption mechanisms of Cu²⁺ in our experimental conditions. On the other hand, in addition to reversible interactions (physisorption), it appeared that irreversible reactions (chemisorption) also took place on the surface of the adsorbent. Results obtained from the intraparticle kinetics model study indicated that intraparticle diffusion is not the limiting step in Cu²⁺ adsorption and that surface adsorption plays a predominant role.

Keywords. Cu²⁺, Removal, Activated carbon, Coconut shells, Dynamic adsorption, Adsorption kinetics.

Manuscript received 8 September 2023, revised 29 December 2023, accepted 18 January 2024.

1. Introduction

The development of chemical, metallurgical and mining industries in the Congo Basin subregion and Gabon in particular, contributes to environmental pollution by heavy metals (Cu, Fe, Mn, Cr, ...) [1,2].

The huge exploitation of these materials is the main cause of the pollution of water resources and soil.

Copper (Cu) for example, in its ionic form, is toxic to species in aqueous media and can cause major health problems in humans. The presence of copper(II) ions (Cu²⁺) at high concentrations in waters, can cause, during repeated exposure or by ingestion, several health problems: anemia, weight loss, breathing difficulties, kidney and liver damages that

*Corresponding author

can lead to death [3]. The World Health Organization (WHO) recommends a limit value for Cu^{2+} of 2 mg/L in drinking water due to its toxicity [4]. Thus, the treatment of industrial and drinking water is important before discharge into the environment and before distribution in the drinking water systems, respectively.

In fact, in industrial environments, wastewater treatment techniques exist. Thus, decantation, flocculation or chemical coagulation [5,6], chemical precipitation [7] and reverse osmosis [8] are among the methods used. These water treatment methods are very expensive and very effective for the removal of organic matter but require additional treatments. In addition, they have limited effectiveness for ionic species, due mainly to the high water solubility and non-biodegradability of these ionic species [9].

On the other hand, adsorption techniques which use porous solids, such as activated carbons (AC), appear to be the least expensive and have fewer disadvantages [10]. These methods have been extensively studied to compensate the shortcomings of other methods used in the treatment of industrial or drinking water [10]. According to the literature, adsorption studies in static (batch) or dynamic conditions have shown that AC-type adsorbents prepared from agricultural waste or biomass with a high carbon content [3,8,11–13] can be used to trap metal ions in aqueous solution. In the case of copper(II) ions, studies under static conditions showed that pH and concentration of the initial solution, mass of adsorbent and contact time, influenced the adsorption capacities at saturation of ACs [3,14–21]. In addition, the kinetic studies have shown that the pseudo-second-order kinetic model appears most suitable to describe the adsorption kinetics of copper(II) ions on ACs in static adsorption mode [18,20–22]. However, very few studies on the elimination and in particular on the adsorption kinetics of copper(II) ions, in dynamic conditions on fixed-bed columns, have been carried out.

Thus, the goal of this work was to valorize waste from coconuts (shells) of the Haut-Ogooué region (Franceville) in Gabon, in the preparation of AC-type adsorbents, thus to carry out dynamic Cu^{2+} adsorption studies in aqueous media on a fixed-bed column under different experimental conditions and subsequently, to study the Cu^{2+} adsorption kinetics on the prepared AC.

2. Experimental

2.1. Preparation of Cu^{2+} solution

A solution of 500 mg/L of Cu^{2+} was prepared by dissolving 1.965 g of copper sulphate pentahydrate salt ($\text{CuSO}_4 \cdot 5\text{H}_2\text{O}$) from LABOSI in a 500 mL volumetric flask. The mixture was stirred for 20 min and thereafter water was added to obtain a solution of concentration 250 mg/L. The latter solution was then used as initial solution for all dynamic adsorption experiments.

2.2. Preparation of activated carbon

The AC preparation method from coconut shells is the same as that used in a recent study [23]. The coconut shells were cleaned, washed several times with distilled water, and then dried at room temperature for 7 days. The dried solids were then crushed, washed with distilled water, dried in an oven for 24 hours (h) at 110 °C and kept in a borosilicate glass crucible. Then, 50 g of the dry material were soaked in a solution of zinc chloride at 1 M (ZnCl_2 : dry material = 1:1 % by weight) for 72 h. The impregnated solid was dried in the oven for 24 h at 110 °C, then heated to 600 °C under air, in a NABERTHEN brand oven, for 1 h and 30 minutes (min) with a rise in temperature of 5 °C/min. The AC obtained was left to cool, rinsed with a solution of HCl (0.1 M), and washed with distilled water until pH of the residual water became neutral. The AC was then dried for 48 h at 110 °C and sieved using a TAMISAR sieve (Standard: AFNOR_NF-X11-501) to obtain different sizes of AC particles.

2.3. Characterizations

Measurements of surface areas and pore volumes were carried out with a Micromeritics TRISTAR 3000 instrument [24]. 100 mg of adsorbent were pretreated for 1 h at 90 °C and 10 h at 350 °C, successively. The nitrogen (N_2) isotherm was acquired at -196 °C. The specific surface area of the AC prepared was determined by means of the Brunauer, Emmett and Teller (BET) theory [25]. Mesoporous and microporous volumes were obtained by the *t*-plot method of De Boer and Dubinin-Radushkevich equations, respectively [26–28].

The pH at the point of zero charge (pH_{pzc}) of the adsorbent prepared was evaluated based on the acid–base titration method [29] and described in a recent study [2]. pH_{pzc} was determined by the point of intersection between the experimental curve and the theoretical curve of $\text{pHf} = f(\text{pHi})$.

Assessments of surface functional groups of the adsorbent were performed using the modified Boehm method [30]. The concentrations (mmol/g) of acid or basic groups were calculated using the following equation:

$$n \text{ (mmol/g)} = \frac{C \times (V_b - V_s) \times 1000}{m_A}$$

where C is the concentration of NaOH or HCl (mol/L); V_b and V_s are the equivalent volumes of the blank and sample (L) respectively; m_A is the mass of adsorbent (g) and 1000 is the conversion factor to mmol.

2.4. Experiments of dynamic adsorption on column

For dynamic adsorption experiments of Cu^{2+} on the prepared AC, we used a Pyrex brand glass column of length 55 cm and diameter 1.4 cm. The protocol and scheme of the experimental set-up were reported in a recent study [2].

During the experiments, various parameters were kept constant: concentration ($C_0 = 250 \text{ mg/g}$), pH of the solution ($\text{pH} = 6.5$) and temperature ($T = 25 \pm 2 \text{ }^\circ\text{C}$). In contrast, particle sizes, heights of adsorbent bed and flow rates were modified according to experiments.

The experiments were stopped when the residual concentrations (C) were equal to the concentrations at the inlet of the column ($C/C_0 = 1$).

The breakthrough curves were established by varying the ratio C/C_0 versus time (t). Exploitation of curve data ($C/C_0 = f(t)$) gives an area (A) in minutes obtained by integration according to the trapeze method [31,32]:

$$A \text{ (min)} = \sum_n \frac{\left(1 - \frac{C_{t_n}}{C_0}\right) + \left(1 - \frac{C_{t_{n+1}}}{C_0}\right)}{2} \times (t_{n+1} - t_n)$$

where C_0 and C are the inlet and outlet concentrations (mg/L) at times t_n and t_{n+1} , respectively.

The Cu^{2+} amounts (q_{ads}) and saturation adsorption capacities (Q_{sat}) were calculated with the following relations [23]:

$$q_{\text{ads}} \text{ (mg)} = D \cdot C_0 \cdot A$$

$$Q_{\text{sat}} \text{ (mg/g)} = \frac{D \cdot C_0 \cdot A}{m_A}$$

with D , C_0 , A , and m_A corresponding to the flow rate (mL/min), the concentration at the inlet of the column (mg/L), the surface area (min) corresponding to the amount of Cu^{2+} adsorbed, and the adsorbent mass used (g), respectively.

Removal percentages (E) of copper(II) ions on the prepared adsorbent were determined by the relation below [23]:

$$E \text{ (%) } = \frac{A}{t_{\text{sat}}} \times 100$$

where t_{sat} is the saturation time (min).

2.5. Adsorption kinetics studies

In order to describe the dynamic behavior and to evaluate the adsorption kinetics of copper(II) ions in adsorption experiments on a fixed-bed column, four mathematical models were applied to the experimental data: the Thomas model, the pseudo-first-order, pseudo-second-order, and intraparticle kinetic models.

2.5.1. Thomas model

The Thomas model [33], described by Sarkar *et al.* and in a recent work [23,34], assumes the Langmuir kinetic model is valid with no mass transfer and axial dispersion during the fixed-bed column adsorption process. It is expressed as:

$$\frac{C}{C_0} = \frac{1}{1 + \exp\left[\left(\frac{k_{Th} \cdot q_e \cdot m_A}{D}\right) - k_{Th} \cdot C_0 \cdot t\right]}$$

The linear form is as below [23,34]:

$$\ln\left(\frac{C}{C_0} - 1\right) = \frac{k_{Th} \cdot q_e \cdot m_A}{D} - k_{Th} \cdot C_0 \cdot t$$

where k_{Th} (mL/(min·mg)) is the Thomas model constant, q_e (mg/g) is the theoretical adsorption capacity, m_A is the adsorbent mass (g), D is the flow rate (mL/min), C_0 is the initial solution concentration (mg/L), and C represents residual (or equilibrium) concentrations at the column outlet (mg/L).

2.5.2. Pseudo-first-, pseudo-second-order, and intraparticle kinetic models

The pseudo-first-order model is described by the following relation [23,35]:

$$\frac{dq_t}{dt} = k(q_e - q_t).$$

By integration between $t = 0$ ($q_t = 0$) and t , the following linear form is obtained:

$$\log(q_e - q_t) = \log(q_e) - \frac{k_1}{2.3} \cdot t$$

where q_t and q_e correspond to maximum adsorption capacities at time t and equilibrium (mg/g), respectively, and k_1 is the adsorption rate constant of the pseudo-first-order kinetic model (min^{-1}).

The pseudo-second-order model is described by the following relation [23,36]:

$$\frac{dq}{dt} = k_2(q_e - q_t)^2.$$

After integration between $t = 0$ and t , the following linear form is obtained:

$$\frac{t}{q} = \frac{1}{k_2 \cdot q_e^2} + \frac{1}{q_e} \cdot t$$

where q_t and q_e correspond to maximum adsorption capacities at time t and equilibrium (mg/g), respectively, and k_2 is the adsorption rate constant of the pseudo-second-order kinetic model ($\text{g}/(\text{mg} \cdot \text{min})$).

According to Webber and Morris [35], the kinetic expression of intraparticle diffusion is described by:

$$q_t = k_d \cdot t^{1/2} + C_d$$

with k_d the intraparticle diffusion rate constant ($\text{mg}/(\text{g} \cdot \text{min}^{1/2})$) and C_d the intercept of the curve. C_d gives an indication of the boundary layer thickness and/or adhesion to the surface [35].

3. Results and discussion

3.1. AC chemical and textural properties

Textural and chemical properties of the prepared adsorbent were evaluated jointly by N_2 physisorption, quantification of the surface functional groups and determination of pH at zero charge point (pH_{pzc}).

Figure 1a presents the N_2 physisorption isotherm. Textural and chemical properties are listed in Table 1. According to IUPAC classification [37], the isotherm obtained is of type I, indicating a microporous material with a hysteresis loop of type H4 which reveals

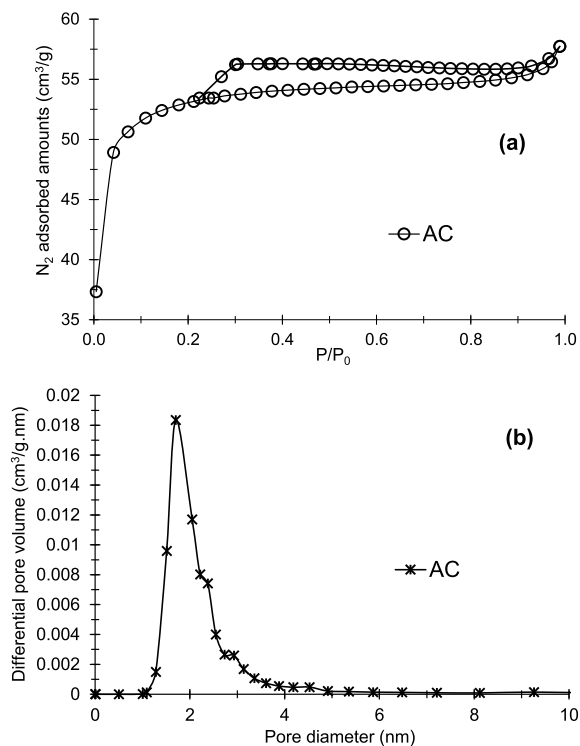


Figure 1. N_2 adsorption–desorption isotherm (a) and pore sizes distribution (b) of prepared activated carbon (AC).

the presence of slit-shaped pores. Results in Table 1 confirm these observations. In fact, the total pore volume ($0.087 \text{ cm}^3/\text{g}$) is very close to the microporous volume ($0.082 \text{ cm}^3/\text{g}$). The average pore size and specific surface area obtained are 1.68 nm and $208.2 \text{ m}^2/\text{g}$, respectively.

Based on the results of N_2 physisorption, the prepared AC shows predominantly a microporous structure.

Results of the chemical properties study from the surface functional group quantification by the Boehm titration method [30] revealed the presence of basic functional groups and phenolic ($-\text{OH}$), lactonic ($-\text{COO}-$), and carboxylic acids ($-\text{COOH}$). Basic functional groups are less abundant than acidic functional groups (Table 1). Moreover, carboxylic acid functional groups (1.45 mmol/g) are more abundant than lactone (1.08 mmol/g) and phenol (0.85 mmol/g) functional groups. Benmahdi *et al.* [38] observed similar results in their work on the synthesis and characterization of microporous

Table 1. Structural and chemical characteristics of prepared activated carbon (AC)

Sample	S_{BET} (m^2/g)	$V_{\text{micro.}}$ (cm^3/g)	$V_{\text{meso.}}$ (cm^3/g)	Average pore size (nm)	pH_{pzc}	Basic functions (mmol/g)	Acidic functions (mmol/g)			
							Total	Carboxyl	Lactone	Phenol
AC	208.2	0.082	0.003	1.68	6.3	0.12	3.39	1.45	1.08	0.86

S_{BET} : specific surface area BET. $V_{\text{micro.}}$: microporous volume. $V_{\text{meso.}}$: mesoporous volume.

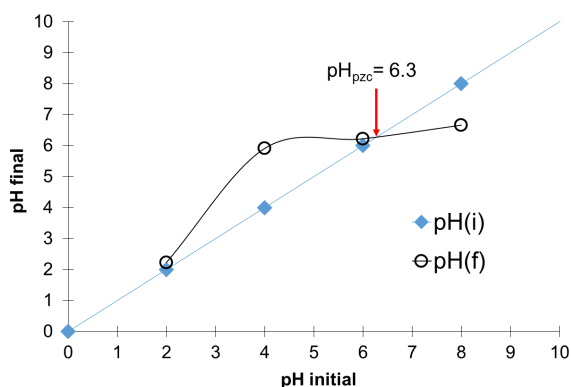


Figure 2. pH_{pzc} determination of prepared activated carbon (AC) using Boehm titration method [30].

granular AC using ZnCl_2 activation. It appears that the activating agent ZnCl_2 promotes the formation of acidic functional groups and microporous structure in the AC preparation.

The evaluated pH_{pzc} of the prepared AC is 6.3 (Figure 2). This acidic value confirms the results obtained on surface functional groups where the acidic functional groups are in majority. In addition, it reveals that the surface of the prepared adsorbent will be positively charged when $\text{pH} < \text{pH}_{\text{pzc}}$, and vice versa [2,38].

Therefore, to increase the number of adsorption sites on the surface of the prepared AC ($-\text{COO}^-$, $-\text{O}^-$, etc.) favorable to Cu^{2+} -AC interactions, the pH of the solution must be greater than pH_{pzc} .

3.2. Dynamic adsorption experiments

The adsorption capacities at saturation and removal percentage of Cu^{2+} were evaluated. Moreover, effects of various parameters on the bed efficiency were studied, including the size (x) of the particles composing the adsorbent bed of the column,

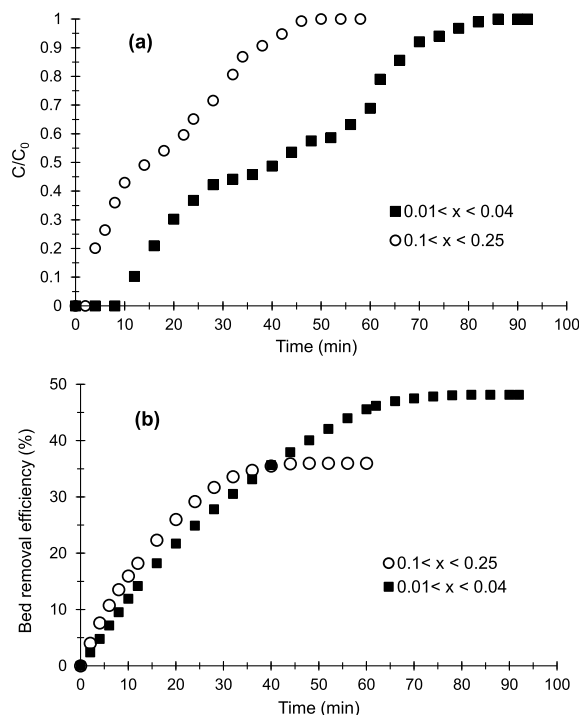


Figure 3. Breakthrough curves (a) and evolution of Cu^{2+} removal efficiency (b) obtained at $25\text{ }^\circ\text{C}$ on the prepared AC with various particle sizes ($h = 1\text{ cm}$, $D = 2\text{ mL/min}$, $C_0 = 250\text{ mg/L}$ and $\text{pH} = 6.5$).

flow rate (D), and bed height (h); and Cu^{2+} adsorption kinetics studies were performed.

3.2.1. Effect of particle size, flow rate and bed height

Two sizes were studied: $0.1 < x < 0.25\text{ mm}$ and $0.01 < x < 0.04\text{ mm}$. Figure 3 shows breakthrough curves (Figure 3a) and the evolution of Cu^{2+} removal efficiency (Figure 3b) obtained.

The breakthrough curves show a multistep adsorption kinetics of Cu^{2+} on the prepared AC according to the time intervals (adsorption zones). The profiles obtained seem to show comparable

adsorption kinetics, diffusion and Cu^{2+} -AC interaction energies on beds of $0.1 < x < 0.25$ mm and $0.01 < x < 0.04$ mm in the first adsorption domain (5–10 min and 10–30 min respectively) and the third zone (35–55 min and 65–95 min respectively). Indeed, the slopes obtained in these zones (Figure 3) are almost similar [39].

However in the second adsorption zone (10–30 min and 30–60 min, respectively), the adsorption kinetics, the diffusions and the adsorption sites strengths are different. The particle bed of $0.01 < x < 0.04$ mm shows slower adsorption kinetics and diffusion of the aqueous phase between grains or in the microporosity with stronger Cu^{2+} -AC interactions on the material surface or in the pores. The slope for $0.01 < x < 0.04$ mm (Figures 3a and 3b) tends more towards the horizontal compared to that for $0.1 < x < 0.25$ mm in the second adsorption zone [25].

In addition, Figures 3a and 3b reveal that the bed with $0.01 < x < 0.04$ mm is more efficient in removing Cu^{2+} . Indeed, the breakthrough (t_p) and saturation (t_{sat}) times obtained (Table 2) on the bed with $0.01 < x < 0.04$ mm (12 and 84 min respectively) are higher than those obtained on the bed with $0.1 < x < 0.25$ mm (4 and 50 min respectively). Also, the results shown in Table 2 indicate that the amounts of Cu^{2+} adsorbed (q_{ads}), the adsorption capacities at saturation (Q_{sat}) and the elimination percentage (E) obtained on the finer particles bed (20 mg; 40.44 mg/g and 48.14%, respectively) are higher than those of the larger particles bed (8.99 mg; 12.85 mg/g and 35.97% respectively). Based on Weber's work [35], this can be explained by the fact that smaller particles have greater flow resistance and a shorter diffusion path in pores or between grains, allowing Cu^{2+} to easily access the surface of AC particles and providing a larger accessible surface area or adsorption sites.

In general, breakthrough curves showed slow adsorption kinetics and diffusion of the aqueous phase between grains, with stronger Cu^{2+} -adsorbent interactions as the adsorbent bed particle size decreases. This allows a better affinity (adsorption) between Cu^{2+} and the prepared AC. In our experimental conditions, the bed composed of the lowest particle sizes ($0.01 < x < 0.04$ mm) appears more efficient in the elimination of Cu^{2+} .

In the study of bed height (h) influence, three bed heights (1; 2 and 3 cm) were studied. Figure 4a

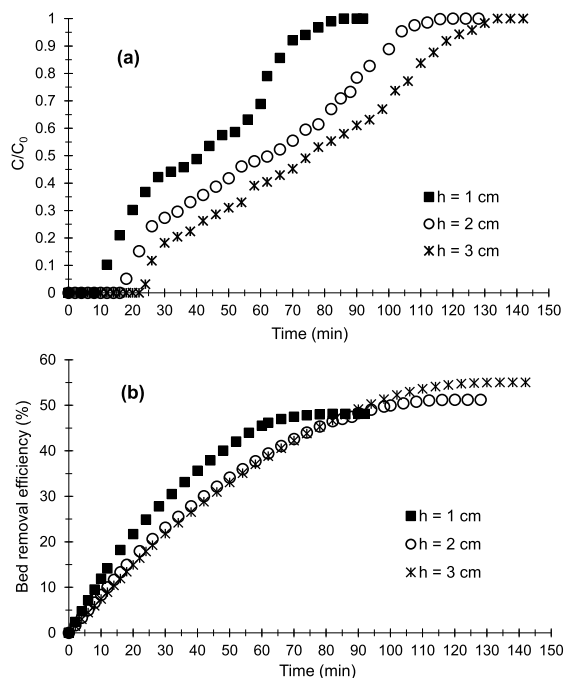


Figure 4. Breakthrough curves (a) and evolution of bed removal efficiency (b) of Cu^{2+} obtained at 25 °C on the prepared AC at various bed heights ($D = 2$ mL/min, $C_0 = 250$ mg/L and $\text{pH} = 6.5$).

shows the breakthrough curves obtained. Regardless of bed height, the multistep adsorption process is always visible on the adsorption profiles obtained. The adsorption kinetics and diffusion of the Cu^{2+} -containing aqueous phase on the surface of the materials or between the grains are comparable for heights 2 and 3 cm (Figures 4a and 4b). On the other hand, in the third adsorption zone for $h = 1$ cm (65–95 min), the Cu^{2+} adsorption kinetics and the diffusion of the aqueous phase are faster compared to those with $h = 2$ and 3 cm (80–105 min and 95–120 min, respectively). Indeed, the slope for $h = 1$ cm tends to be much more vertical compared to that for $h = 2$ and 3 cm (Figure 4a).

Figures 4a and 4b indicate that the bed $h = 3$ cm is more efficient in removing Cu^{2+} . Indeed t_p (24 min) and t_{sat} (134 min) obtained are higher than those obtained with beds $h = 2$ and 1 cm (Table 2). In addition, q_{ads} , Q_{sat} and E obtained with $h = 3$ cm (36.87 mg; 52.52 and 55.02%) are higher than those with $h = 2$ and 1 cm as summarized in Table 2.

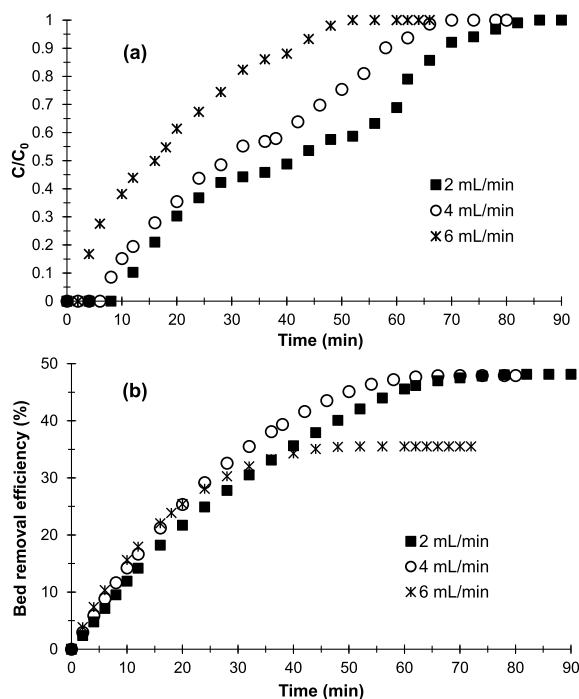
Table 2. Experimental results of Cu^{2+} removal in aqueous media on the prepared AC at 25 °C and under different experimental conditions

Parameters	Experimental conditions	t_c (s)	t_p/t_{sat} (min)	q_{ads} (mg)	Q_{sat} (mg/g)	E (%)
Particle sizes (mm)	$0.01 < x < 0.04$	46.18	12/84	20.22	40.44	48.14
	$0.1 < x < 0.25$		4/50	8.99	12.85	35.97
Bed heights h (cm)	1	46.18	12/84	20.22	40.44	48.14
	2	92.36	18/120	30.74	46.23	51.23
	3	135.54	24/134	36.87	52.52	55.02
Flow rates D (mL/min)	2	46.18	12/84	20.22	40.44	48.14
	4	23.09	8/68	24.44	30.55	47.92
	6	15.39	4/52	27.23	19.79	35.49

This could be explained by the fact that an increase in h leads to an increase in the accessible surface area of the adsorbent and a greater dispersion of adsorption sites favorable to Cu^{2+} -AC interactions. Similar results were observed in the work of Hasfalina *et al.* [39] and Kavianinia *et al.* [40]. Thus, the higher the adsorbent bed, the more efficient the bed becomes in removing Cu^{2+} under our operating conditions.

Regarding the influence of flow rate (D), 2; 4 and 6 mL/min were flow rates studied. Based on Figure 5a, the multistep adsorption mode disappears when D increases. With 6 mL/min, a single-step adsorption is visible. It seems that the diffusion of the Cu^{2+} -containing aqueous phase is rapid between grains and therefore limits the Cu^{2+} -AC interactions.

The results in Table 2 show that when D increases, q_{ads} , Q_{sat} and E decrease. These results also indicate that the prepared AC is more effective in removing Cu^{2+} when the applied flow rate is 2 mL/min. Indeed, Q_{sat} and E obtained with 2 mL/min (40.44 mg/g and 48.14%, respectively) are higher than those obtained with 4 mL/min (30.55 mg/g and 47.92%, respectively) and 6 mL/min (19.79 mg/g and 35.49%, respectively). The decrease in E at higher flow rates is due to the decrease in contact time (Table 2) between the Cu^{2+} -containing aqueous phase and the adsorbent. This resulted in low diffusion of adsorbate into the surface or rapid diffusion between the grains of the adsorbent bed [41]. Chen *et al.* [21] observed similar results in their studies concerning the effect of contact time on the removal of copper ions in an aqueous solution on ACs.

**Figure 5.** Breakthrough curves (a) and evolution of Cu^{2+} removal efficiency (b) obtained at 25 °C on the prepared AC at various flow rates ($h = 1$ cm, $C_0 = 250$ mg/L and $\text{pH} = 6.5$).

Based on results of the influence of flow rates, it appears that increasing the flow rate decreases the efficiency of the prepared AC in Cu^{2+} removal. In our experimental conditions, 2 mL/min is the optimal flow rate.

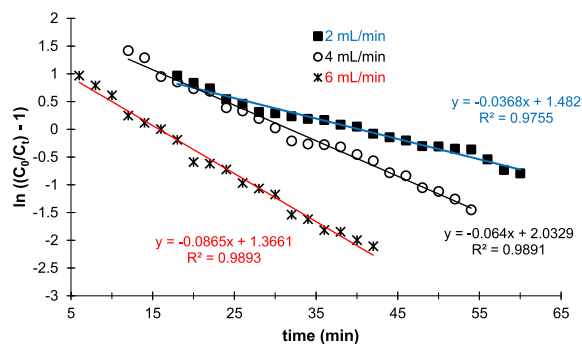


Figure 6. Linear plots of the Thomas kinetic model applied to experimental data of Cu^{2+} removal on the prepared AC at various flow rates.

3.2.2. Adsorption kinetics studies

Adsorption kinetics studies were carried out on experiments performed on the influence of flow rates. Several kinetics models (Thomas, pseudo-first-, pseudo-second-order and intraparticle) were applied to experimental data in this study.

Figure 6 shows the linear plots after application of the Thomas linear model. According to these profiles, the experimental points are in agreement with the model. Indeed, the linear regression coefficients R^2 of each curve are very close to 1 (Table 3).

In addition, the calculated capacities at saturation ($Q_{e, \text{Cal}}$) are close to the experimental capacities ($Q_{e, \text{exp}}$) as summarized in Table 3. In particular for the linear plot obtained with 2 mL/min, $Q_{e, \text{exp}}$ and $Q_{e, \text{cal}}$ are 40.44 and 40.27 mg/g, respectively. Based on these results and according to the Thomas model, external and internal diffusion limitations are non-existent in the Cu^{2+} adsorption experiments performed, the driving force follows the Langmuir isotherm and the reaction kinetics is reversible. Thus, Cu^{2+} adsorption on the prepared AC is limited by physical interactions or physisorption, but it is controlled by mass transfer at the interface.

Figure 7 shows the linearization of the pseudo-first- (Figure 7a) and pseudo-second-order kinetic models (Figure 7b) applied to experimental data for Cu^{2+} adsorption. According to the results of linearization, both kinetic models are in good agreement with the experimental points. The linear regression coefficients R^2 obtained in both cases are

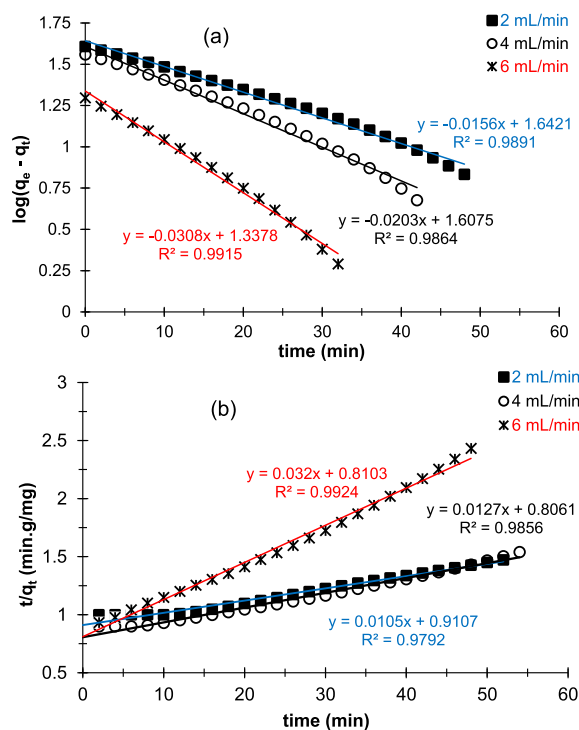


Figure 7. Linear plots of pseudo-first-order (a) and pseudo-second-order (b) kinetic models applied to experimental data of Cu^{2+} removal on the prepared AC at various flow rates.

all close to 1 (Table 3). The results indicate that we have two types of interactions on the surface of the prepared AC: chemisorption and physisorption. These results differ from those of Chen et al. [21] obtained during their work on kinetic adsorption studies of copper(II) ions on ACs in an aqueous media by batch adsorption.

However, the calculated capacities at saturation ($Q_{e, \text{cal}}$) according to the pseudo-second-order kinetic model are very high compared to the experimental values ($Q_{e, \text{exp}}$). In contrast, $Q_{e, \text{cal}}$ obtained with the pseudo-first-order kinetic model is close to the values of $Q_{e, \text{exp}}$ (Table 3).

It therefore seems that the pseudo-first-order kinetic model is the model that best describes the adsorption kinetics of copper(II) ions on the prepared AC in our experimental conditions. On the other hand, in addition to reversible interactions (physisorption), it seems that irreversible reactions (chemisorption) also take place on the surface of

Table 3. Parameters of the Thomas, pseudo-first-order, pseudo-second-order, and intraparticle kinetic models of Cu^{2+} adsorption ions on the prepared AC

<i>D</i> (ml/min)	Experimental data		Thomas model		Pseudo-first-order		Pseudo-second-order			Intraparticle			
	$Q_{e \text{ exp}}$ (mg/g)	$Q_{e \text{ cal}}$ (mg/g)	$k_{Th} \times 10^{-3}$ mL/(mg·min)	R^2	$Q_{e \text{ cal}}$ (mg/g)	$k_1 \times 10^{-4}$ (1/min)	R^2	$Q_{e \text{ cal}}$ (mg/g)	$k_2 \times 10^{-6}$ (g/(mg·min))	R^2	K_d (mg/(min ^{1/2} ·g))	C_d	R^2
2	40.44	40.27	147	0.976	43.86	359	0.989	95.24	121	0.979	6.05	8.54	0.998
4	30.55	31.76	257	0.989	40.50	467	0.986	78.74	200	0.986	5.93	7.32	0.997
6	19.79	15.79	346	0.989	21.76	708	0.992	31.25	1364	0.992	3.67	2.83	0.992

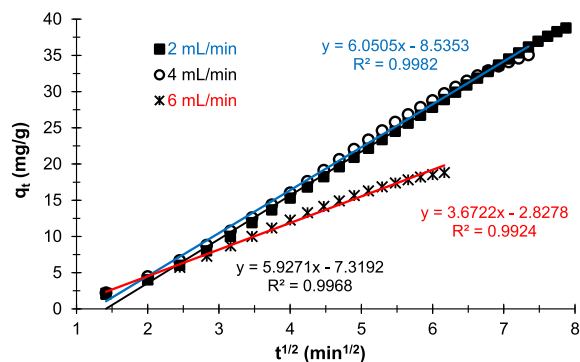


Figure 8. Intraparticle kinetic model applied to experimental data of Cu^{2+} removal on the prepared AC at various flow rates.

the adsorbent. Chemisorption, also known as chemical adsorption, involves the formation of chemical bonds. In other words, it is mainly based on interactions of a covalent nature, i.e., involving the formation of a bond between the adsorbate and the adsorbent, the effects of which are often irreversible [42]. In our experimental conditions ($\text{pH} = 6.5$), the products of chemical reactions at the surface of the adsorbent appear to be the CuO copper oxide [43,44].

Figure 8 shows the linear plots obtained after application of the intraparticle model to the Cu^{2+} adsorption data on the prepared adsorbent. Results show that regardless of the flow rate applied, the linear plots do not pass through the origin ($C_d \neq 0$). According to this model [35,45], in our experimental conditions, intraparticle diffusion is involved in the Cu^{2+} adsorption mechanism on the prepared AC. Thus, it is not the limiting step and the only process controlling Cu^{2+} adsorption.

On the other hand, the linear regression coefficients R^2 obtained for each plot are close to 1 (Table 2). Therefore, intraparticle diffusion plays an important role in the process (mechanism) of Cu^{2+} adsorption on the prepared AC in our experimental conditions [23]. Also, the intercept curve (C_d) informs on the boundary layer thickness. The higher the C_d values, the greater the contribution to surface grip in the speed-limiting step [45]. The results in Table 3 indicate that the lower the flow rate, the greater the adhesion of Cu^{2+} to the surface of the prepared adsorbent. However, regardless of the flow rate

applied, the C_d values obtained are very high. This confirms that intraparticle diffusion is not the limiting step in Cu^{2+} adsorption on the prepared AC and that surface adsorption plays a predominant role in our experimental conditions.

4. Conclusion

This work aimed to prepare an activated carbon (AC) from coconut shells collected in Franceville in the Haut-Ogooué region (Gabon) with the activating agent ZnCl_2 . Then we carried out dynamic adsorption experiments of copper(II) ions (Cu^{2+}) on fixed-bed columns in aqueous media at different experimental conditions, in order to determine optimal conditions for Cu^{2+} removal. Studies of Cu^{2+} adsorption kinetics were also performed.

Textural and chemical characterizations of the prepared AC revealed a predominantly microporous structure with a microporous volume of $0.082 \text{ cm}^3/\text{g}$, an average pore size of 1.68 nm , a specific surface area (S_{BET}) of $208.4 \text{ m}^2/\text{g}$ and a pH at the point of zero charge (pH_{pzc}) of 6.3 . Here, acid functional groups (carboxylic acid, phenol and lactone) are in majority on the surface of the prepared AC.

In dynamic adsorption experiments, it appears that the particle size (x) of the column bed, flow rate (D) and bed height (h) influence adsorption capacities at saturation (Q_{sat}) and Cu^{2+} removal percentages on the prepared AC. The best Q_{sat} and E (52.52 mg/g and 55.02% respectively) were obtained with $0.01 < x < 0.04 \text{ mm}$, $D = 2 \text{ mL/min}$ and $h = 3 \text{ cm}$ with Cu^{2+} concentration and pH constant (250 mg/L and 6.5 , respectively).

Kinetic studies indicated that the Thomas and pseudo-first-order kinetics model best describe the mechanisms of Cu^{2+} adsorption in our experimental conditions. On the other hand, in addition to reversible interactions (physisorption), it appeared that irreversible reactions (chemisorption) also took place on the surface of the prepared adsorbent. Results from the intraparticle kinetic model indicate that intraparticle diffusion is not the limiting step in Cu^{2+} adsorption and that Cu^{2+} surface adsorption on the prepared AC plays a predominant role. Based on the results, the prepared AC could be used as adsorbent in depollution of aqueous media with low concentrations of copper(II) ions.

Declaration of interests

The authors do not work for, advise, own shares in, or receive funds from any organization that might benefit from this article, and have declared no affiliation other than their research organizations.

Acknowledgments

The authors are grateful to Professor Samuel Mignard and the CNRS Research Fellow Alexander Sachse of the Institute of Media and Materials Chemistry of Poitiers (IC2MP) for their help in the surface characterization of activated carbon.

References

- [1] K. M. Emmanuel, M. K. Joëlle, K. K. Urbain, L. N. Albert, M. M. Mia, *Int. J. Innov. Appl. Stud.*, 2019, **27**, 728-741.
- [2] M. M. Charly, T.-M. Pradel, N. Francis, M. Berthy Lionel, B. M. Spenseur, S. Alexander, M. Samuel, F. T. Guy Raymond, *J. Environ. Pollut. Hum. Health*, 2022, **10**, 58-70.
- [3] A. Haluk, B. Yasemin, Y. Ciğdem, *J. Environ. Manage.*, 2008, **87**, 37-45.
- [4] Organisation Mondiale de la Santé (OMS), "Soixante-quatrième assemblée mondiale de la santé, Rapport du secrétariat: Stratégies pour la gestion sans risque de l'eau de boisson destinée à la consommation humaine, A64/24", 2011.
- [5] A. G. Patrick, A. N. Blaise, D. B. Kouamé, K. D. Ouattara, G. K. Gildas, T. Albert, *Int. J. Innov. Sci. Res.*, 2015, **13**, 530-541.
- [6] N. Abdullah, N. Yusof, W. J. Lau, J. Jaafar, A. F. Ismail, *J. Ind. Eng. Chem.*, 2019, **76**, 17-38.
- [7] B. Mohamed, *Arab. J. Chem.*, 2011, **4**, 361-377.
- [8] H. A. Al-Aoh, *Desalin. Water Treat.*, 2019, **170**, 101-110.
- [9] C. Y. Yin, M. K. Aroua, W. M. Ashri, W. Daud, *Chem. Eng. J.*, 2009, **184**, 8-14.
- [10] M. A. Elias, H. Tony, S. Palanivel, *Environ. Chem. Ecotoxicol.*, 2021, **3**, 1-7.
- [11] M. H. A. Meshari, H. A. AL-Aoh, *Mater. Res. Express*, 2021, **8**, article no. 035012.
- [12] W. Li, J. Peng, L. Zhang, H. Xia, N. Li, K. Yang, X. Zhu, *Crops Prod.*, 2008, **28**, 73-80.
- [13] K. J. Cronje, K. Chetty, M. Carsky, J. N. Sahu, B. C. Meikap, *Desalination*, 2011, **275**, 276-284.
- [14] Y. Y. Augustin, K. A. Narcisse, A. Kopoin, K. Y. Benjamin, *Afr. Sci.*, 2018, **14**, 38-47.
- [15] M. H. Chen, R. Z. Maryam, L. C. Abdullah, M. Rashid, *APCBEE Proc.*, 2012, **3**, 255-263.
- [16] N. D. Tumin, A. L. Chuah, Z. Zawani, S. A. Rashid, *J. Eng. Sci. Technol.*, 2008, **3**, 180-189.
- [17] K. N. Arsène, G. A. Patrick, D. K. Ouattara, T. Albert, *Rev. Ivoir. Sci. Technol.*, 2017, **29**, 44-54.
- [18] A. T. Sabah, *Aquat. Sci. Technol.*, 2013, **1**, 53-77.
- [19] V. T. Thuan, T. P. B. Quynh, D. N. Trinh, N. T. H. Le, L. G. Bach, *Adsorpt. Sci. Technol.*, 2017, **35**, 72-85.
- [20] D. Erhan, D. Nadir, T. S. Maral, K. Mehmet, *Chem. Eng. J.*, 2009, **148**, 480-487.
- [21] W. S. Chen, Y. C. Chen, C. H. Lee, *Processes*, 2022, **10**, article no. 150.
- [22] H. Demiral, C. Güngör, *J. Clean. Prod.*, 2016, **124**, 103-113.
- [23] M. M. Charly, N. Francis, T. M. Pradel, M. Berthy Lionel, B. M. Spenseur, F. T. Guy Raymond, *Open J. Inorg. Chem.*, 2023, **13**, 25-42.
- [24] L. A. Amola, T. Kamgaing, D. R. T. Tchuifon, C. D. Atemkeng, S. G. Anagho, *J. Mater. Sci. Chem. Eng.*, 2020, **8**, 53-72.
- [25] B. Thomas, M. M. Charly, M. Samuel, P. Yannick, *Microporous Mesoporous Mater.*, 2013, **182**, 109-116.
- [26] S. Brunauer, P. H. Emmett, E. J. Teller, *J. Am. Chem. Soc.*, 1938, **60**, 309-319.
- [27] B. C. Lippens, J. H. De Boer, *J. Catal.*, 1965, **4**, 319-323.
- [28] J. Lynch, F. Raatz, P. Dufresne, *Zeolites*, 1987, **7**, 333-340.
- [29] J. H. De Boer, B. C. Lippens, B. G. Lisen, B. C. P. Broekhoff, A. Van Den Heuvel, T. J. Osinga, *J. Colloid Interface Sci.*, 1966, **21**, 405-414.
- [30] H. P. Boehm, *Adv. Catal.*, 1966, **16**, 179-274.
- [31] M. M. Charly, T. M. Pradel, N. Francis, B. Thomas, M. Samuel, *Am. J. Environ. Prot.*, 2022, **10**, 83-90.
- [32] M. M. Charly, N. Francis, T. M. Pradel, E. E. Ferdinand, B. B. N. Landry, B. Thomas, M. Samuel, *J. Environ. Prot.*, 2023, **14**, 66-82.
- [33] C. Thomas Henry, *J. Am. Chem. Soc.*, 1944, **66**, 1664-1666.
- [34] S. Sarkar, N. Bar, S. K. Das, *J. Environ. Eng. Land. Manage.*, 2022, **30**, 331-341.
- [35] W. Junior, in *Adsorption in Physicochemical Process for Water Quality Control* (R. L. Metcalf, J. N. Pitts, eds.), vol. 5, Wiley Interscience, New York, 1972, 199-259.
- [36] Y. S. Ho, G. McKay, *Process Biochem.*, 1999, **34**, 451-465.
- [37] IUPAC, *Pure Appl. Chem.*, 1985, **57**, 603-619.
- [38] B. Fatiha, O. Kafra, K. Sami, K. Mounira, M. C. Odile, *Fuller. Nanotub. Carbon Nanostructures*, 2021, **29**, 657-669.
- [39] C. M. Hasfalina, R. Z. Maryam, C. A. Luqman, M. Rashid, *APCBEE Proc.*, 2012, **3**, 255-263.
- [40] K. Iman, G. P. Paul, G. K. Nadia, R. K. H. David, *Carbohydr. Polym.*, 2012, **90**, 875-886.
- [41] R. Lakshmi, G. Balaji, I. Rico, H. Hamad, *Adsorpt. Sci. Technol.*, 2021, **2021**, 251-259.
- [42] L. Lee, *Fundamentals of Adhesion*, vol. 6, Springer Science & Business Media, New York, 2013.
- [43] M. J. N. Pourbaix, *Atlas of Electrochemical Equilibria in Aqueous Solutions*, Gauth-Villa, 1966.
- [44] O. Abollino, M. Aceto, M. Malandrino, C. Sarzanini, E. Mentastì, *Water Res.*, 2003, **37**, 1619-1627.
- [45] E. Malkoc, N. Yasar, *J. Hazard. Mater.*, 2006, **135**, 328-336.